Journal of Experimental Marine Biology and Ecology 497 (2017) 1–10

Contents lists available at ScienceDirect

Journal of Experimental Marine Biology and Ecology

journal homepage: www.elsevier.com/locate/jembe

Pneumatocysts provide buoyancy with minimal effect on drag for kelp in wave-driven flow

Nicholas P. Burnett*, M.A.R. Koehl

Department of Integrative Biology, University of California, Berkeley, CA 94720, United States

ARTICLE INFO

Keywords:
Egregia menziesii
Pneumatocysts
Buoyancy
Waves
Kelp
Hydrodynamics

ABSTRACT

Many seaweeds have buoyant gas-filled bladders (pneumatocysts) that hold fronds upright in the water column and enhance their access to light for photosynthesis. However, ambient water currents bend flexible seaweeds, pushing fronds closer to the substratum where light is lower, so the hydrodynamic drag on pneumatocysts may counteract their buoyancy in flowing water. The effects of pneumatocysts on frond hydrodynamic drag were investigated in this study, as well as how the positions of pneumatocysts along fronds affect their motion and height in wave-driven water flow. The kelp *Egregia menziesii* was used as a model organism because it is abundant on wave-swept rocky shores and because our field surveys revealed that this species shows great variation in pneumatocyst size, number, and location on fronds. In laboratory towing-tank studies, it was found that drag on pneumatocysts was reduced when they were bent over by flowing water. The drag due to pneumatocysts was small compared to the drag on a whole frond. At flow speeds up to 0.58 m s^{-1}, the buoyant force exerted by a pneumatocyst was greater than the drag it experienced. In wave-tank experiments using models of fronds with pneumatocysts at different positions, the pneumatocysts were most effective at lifting fronds high in the water column when they were located at the distal tips of the fronds, both in small and large waves. However, if fronds had pneumatocysts that were not at the tip, an increase in the peak velocities of waves led to an increase in the heights of the fronds in the water column. In the field, pneumatocysts did not affect the back-and-forth horizontal motion of *E. menziesii* exposed to waves, but fronds with pneumatocysts were higher in the water column than fronds with no pneumatocysts, even when the number of pneumatocysts on a frond was low. Our results indicate that pneumatocysts can exhibit great variability in size, number, and location with only a small effect on hydrodynamic forces on a kelp, that pneumatocysts at frond tips are most effective at holding kelp high in the water column, but that only a few pneumatocysts at any location along a frond can enhance the frond's height in waves.

1. Introduction

The intertidal zones of many temperate rocky shores are populated by large seaweeds whose abundance is highly correlated with increased biodiversity because they serve as a food source and habitat for many other organisms (e.g., Abbott and Hollenberg, 1976; Graham, 2004; Christie et al., 2009). Moving water from ocean currents and waves impose hydrodynamic forces on the seaweeds (e.g., Koehl, 1984; Denny, 1988; Gaylord, 1999). On the west coast of North America, waves generally have periods between 8 and 20 s (NOAA Buoy Center, www.ndbc.noaa.gov), resulting in thousands of waves each day that move onto the shore and exert forces on the seaweeds. If the magnitudes of the forces exceed the seaweed strength, the seaweeds can be dislodged from the substratum or suffer a partial breakage of the thallus (Koehl and Wainwright, 1977; Carrington, 1990; Demes et al., 2013), resulting in the removal of the seaweed and its epibiota from the ecosystem (Krumhansl and Scheibling, 2012).

The morphological and mechanical traits of a seaweed can alter the hydrodynamic forces it experiences. A seaweed with a flexible thallus can be reconfigured by moving water into a small, streamlined shape that reduces hydrodynamic forces on the seaweed (Koehl, 1984; Carrington, 1990; Martone et al., 2012). In back-and-forth wave-driven flow, flexible seaweeds move with the water in the direction of flow, thus the water velocity relative to the seaweed is reduced and hydrodynamic forces on the seaweed are lower than they would be if the seaweed were rigid (Koehl, 1986). However, moving with the ambient water motion may not always minimize forces on the seaweed: when the seaweed becomes fully extended it can experience inertial loading (i.e., “jerk” sensu Denny et al., 1998) due to the sudden thallus deceleration, in addition to the hydrodynamic forces from water that

---

* Corresponding author.
E-mail address: burnettnp@berkeley.edu (N.P. Burnett).

http://dx.doi.org/10.1016/j.jembe.2017.09.003
Received 13 July 2017; Received in revised form 31 August 2017; Accepted 7 September 2017

continues moving past the seaweed (Koehl, 1986).

Many flexible seaweeds rely on buoyancy to remain upright in the water column and to access light for photosynthesis (e.g., Stewart et al., 2007). When hydrodynamic forces become sufficiently large, a buoyant seaweed can be pushed closer to the substratum, but return to its upright position once the water motion slows (Stewart, 2004). Unidirectional currents moving along shore can re-orient buoyant seaweeds with the current, reducing the magnitude of the hydrodynamic forces the seaweeds experience from waves moving toward the shoreline (Gaylord et al., 2003). Buoyancy has also been shown to interfere with the passive reconfiguration of a seaweed into a compact, streamlined shape when in flowing water, and thus buoyancy counteracts this mechanism of hydrodynamic force reduction (Stewart, 2006a).

The buoyancy of many species of seaweeds is provided by gas-filled bladders (pneumatocysts), which have a variety of forms across seaweed taxa (Abbott and Hollenberg, 1976). For example, *Nereocystis luetkeana* has a single, large pneumatocyst at the end of its stipe, whereas *Macrocystis pyrifera* has numerous small pneumatocysts at regular intervals along the thallus, with pneumatocysts near the holdfast being larger than more distal pneumatocysts. Most studies of the biomechanics and hydrodynamics of seaweed buoyancy have focused on small species (thallus < 0.5 m in length; pneumatocysts smaller than 2 cm in diameter) to investigate the trade-off between the flexibility of the whole thallus and pneumatocyst buoyancy (e.g., Stewart, 2004, 2006a,b; Stewart et al., 2007). However, little is known about the influence of pneumatocysts on the forces on and movement of large seaweeds (thallus longer than 1 m) in ambient flow. Furthermore, the consequences to drag of the size and deformability of a pneumatocyst have not been explored, and the effects of the positions of pneumatocysts along fronds on the behavior of seaweeds in flowing water are not understood. Understanding basic principles about how buoyant pneumatocysts affect the hydrodynamic forces on and movement of large, flexible structures, such as ecologically-important seaweeds, can not only improve predictions of how those seaweeds will be affected (e.g., growth, damage, dislodgement) by changes in flow conditions (e.g., increased frequency of storms) or by other environmental factors that can directly damage the pneumatocysts (e.g., herbivory, abrasion against the substratum).

We used the feather boa kelp, *Egregia menziesii*, to study the hydrodynamic consequences of having pneumatocysts of different sizes, numbers, and locations along the thallus of a long seaweed. *E. menziesii*, which is one of the largest species of kelp abundant in the rocky intertidal zone along the west coast of North America from Baja California to southeast Alaska, has numerous strap-like fronds that grow to lengths of 3 m or more from a perennial holdfast (Abbott and Hollenberg, 1976) (Fig. 1A). The rachis of each frond (about 1 to 2 cm wide) bears ellipsoidal pneumatocysts (up to 5 cm long) and narrow lateral blades (up to 5 cm long) along both edges (Henkel and Murray, 2007) (Fig. 1B).

The objective of the present study was to determine how the number, size, flexibility, and location of pneumatocysts on long kelp fronds affect the motion of and hydrodynamic forces on the fronds in wave-driven water flow. The specific questions investigated were: (1) How abundant are pneumatocysts on the fronds of *Egregia menziesii*, and do their abundances change with season? Where do pneumatocysts occur on the fronds and how large are those pneumatocysts? How variable are the locations, numbers, and sizes of pneumatocysts between individuals? (2) What is the magnitude of the hydrodynamic force on a single pneumatocyst, and how do the size and the reconfiguration of a pneumatocyst in moving water affect the force on the pneumatocyst? (3) How much do pneumatocysts increase the drag on a frond? (4) How does the location of pneumatocysts on a frond affect the depth of the frond in the water column under different wave conditions? (5) How do pneumatocysts in natural arrangements on kelp in the field affect the horizontal movement and depth of fronds in ambient waves?

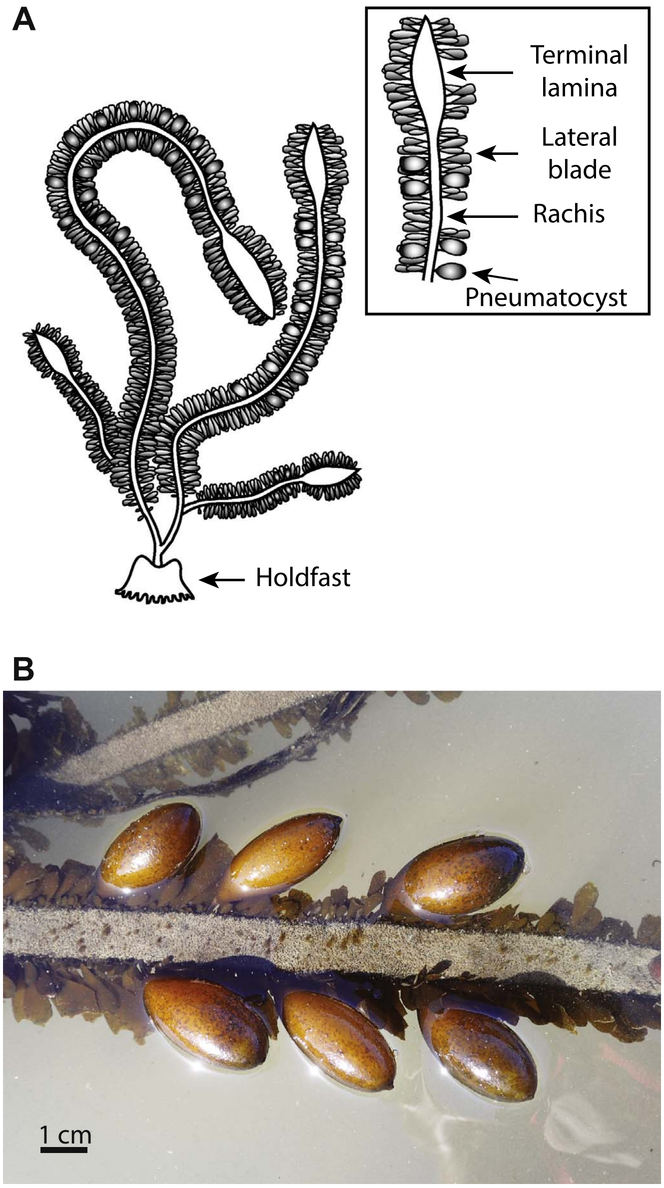

Fig. 1. (A) Anatomy of an *Egregia menziesii* sporophyte. Individual fronds on the kelp are strap-like and can grow to > 3 m in length. (B) Each frond's rachis bears lateral blades and ellipsoidal pneumatocysts along both edges.

2. Methods

2.1. Pneumatocyst surveys

2.1.1. Field sites

Pneumatocysts on *Egregia menziesii* were surveyed at four rocky intertidal sites in northern California. Two moderately wave-exposed sites were located near Bodega, CA, USA: Horseshoe Cove (HC) (38°18′59″ N, 123°4′12″ W) and Miwok Beach (MW) (38°21′25″ N, 123°4′2″ W). Two wave-exposed sites were located in the Point Reyes National Seashore, CA, USA: Kehoe Beach (KB) (38°9′56.08″ N, 122°57′6.04″ W) and McClures Beach (MC) (38°11′2.70″ N, 122°58′2.33″ W). Waves were attenuated as they moved across the wide, gently-sloping surf zones at HC and MW, whereas the steep rocky faces at KB and MC were hit by bigger, unattenuated waves (Denny, 1995; Johnson et al., 2015a,b). Furthermore, the fauna colonizing *E. menziesii* at HC and MW are dominated by herbivorous invertebrates, and the fauna colonizing *E. menziesii* at KB and MC are dominated by sessile suspension feeders (Burnett, 2017). These communities are consistent with similar wave exposure gradients observed at other sites (Underwood et al., 1983; Bertness et al., 2006).

2.1.2. Abundance of pneumatocysts

The abundance of pneumatocysts on the fronds of intertidal *E. menziesii* were surveyed at HC, KB, and MC in February and June 2016. At each site, kelp were surveyed along a horizontal transect through the *E. menziesii* zone (low intertidal), selecting every third individual that was encountered. The lengths of all the fronds on the selected kelp were measured to the nearest 1 cm, and the number of pneumatocysts on each frond was recorded. Within each survey, as many kelp as possible were measured along the transect until the rising tide and waves re-immersed the kelp. The numbers of pneumatocysts on the fronds were compared between the two seasons at each site using Mann-Whitney *U* tests.

2.1.3. Location of pneumatocysts

The locations of pneumatocysts on the fronds of *E. menziesii* were measured at MW and MC in July 2017. At each site, kelp were surveyed, as described above. One frond from each kelp was haphazardly selected, and locations of all pneumatocysts longer than 0.5 cm on the frond, as well as the total length of the frond, were measured to the nearest 1 cm. For each frond, the locations of the proximal-most and distal-most pneumatocysts, relative to the position on the kelp at which the frond branches from the holdfast or another frond, were calculated from the survey data. The relative locations of the fronds were compared between the two sites using a Mann-Whitney *U* test.

2.1.4. Size of pneumatocysts

The sizes of pneumatocysts on the fronds of intertidal *E. menziesii* were surveyed at MW and MC in September 2016. At each site, ten kelp were selected by following the protocol for kelp surveys, as described above (i.e., approximately every third kelp along a horizontal transect was selected). All the pneumatocysts on each kelp were removed, bagged according to the individual kelp, and then photographed. The planform area of each pneumatocyst was measured to the nearest 0.01 cm^2 using ImageJ software (ImageJ, v.1.47, National Institutes of Health, USA). The sizes of pneumatocysts were compared between the two sites using a Mann-Whitney U test.

2.2. Reconfiguration and drag on pneumatocysts

To determine the reduction in drag resulting from the reconfiguration of a pneumatocyst, we compared the drag on pneumatocysts that could bend over in flow with the drag on pneumatocysts that did not reconfigure in flow because their petioles had been stiffened by reinforcing the petiole with foil. Similarly, the effect of pneumatocyst buoyancy on reconfiguration and drag was determined by comparing intact gas-filled pneumatocysts with those that had been punctured and filled with water. The reconfiguration of and drag on individual pneumatocysts were measured before and after the pneumatocyst's buoyancy or the stiffness of the pneumatocyst's petiole was changed. Individual fronds with pneumatocysts were collected from MW and MC in January and February 2016. Fronds were cut into sections (length = 10 cm) with a single pneumatocyst in the middle of each section, and all lateral blades (Fig. 1A) were trimmed away (Fig. 2). Lateral blades were trimmed away to isolate the forces acting on the pneumatocyst by itself, and because preliminary observations of pneumatocysts and lateral blades in the field showed that the size and presence of pneumatocysts was not dependent on the presence, abundance, and size of lateral blades. The pneumatocysts were grouped into one of two treatments, and all pneumatocysts within each group originated from separate kelp. In one group, each pneumatocyst's petiole was stiffened by reinforcing the petiole with a short length of aluminum foil. In the second group, the pneumatocyst was punctured and filled with water, rendering it neutrally buoyant (Stewart, 2004). The fronds and their pneumatocysts were towed through a tank of water (working section with a cross-section = 30 × 30 cm, length = 100 cm) at a constant velocity (mean = 0.58 m s^{-1}, see Results), and a spring scale was used to measure drag on the fronds and pneumatocysts (Ohaus Model 8261-M, Pine Brook, NJ, USA). While the fronds were towed through the water, the fronds and pneumatocysts were videotaped at 50 frames per second (Fastec Imaging, San Diego, CA, USA). The deflection angle of the pneumatocysts in each frame of the videos was measured to the nearest 0.01° using ImageJ and calculated using the law of cosines from fundamental trigonometry, which describes any triangle with three known side lengths (Lial et al., 2009):

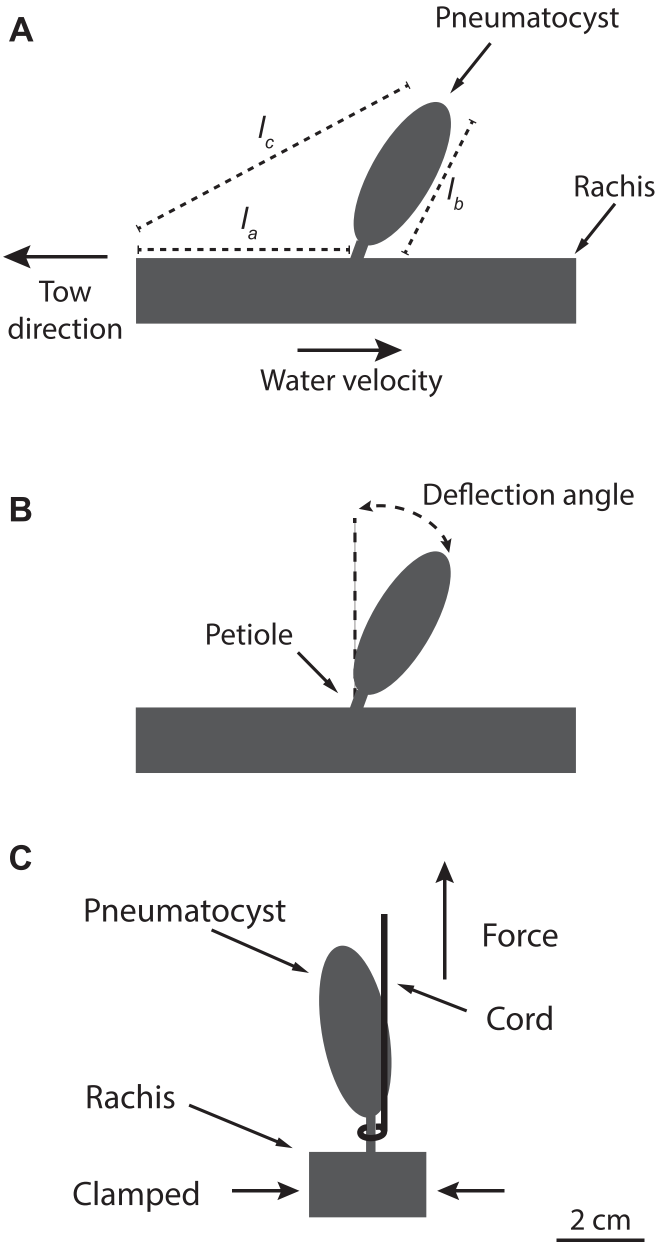

Fig. 2. Towing set-up of a pneumatocyst attached to a rachis with the lateral blades removed. The frond is towed from right to left, so the water flow relative to the frond is from left to right. (A) Distances (l_a, l_b, l_c) between three points on the frond and pneumatocyst. (B) Deflection angle of the pneumatocyst (Eq.(1)), measures how far the pneumatocyst re-oriented in flowing water from an orientation perpendicular to the edge of the rachis. (C) The force to break a pneumatocyst from the frond was measured by tying a nylon cord around the pneumatocyst's petiole and clamping the frond in the Instron materials testing machine. The cord was then pulled vertically, while measuring the force on the pneumatocyst, until the pneumatocyst broke from the frond.

$$Deflection\ (^{\circ}) = \cos^{-1}\left(\frac{l_a^2 + l_b^2 - l_c^2}{2 l_a l_b}\right) - 90^{\circ} \tag{1}$$

where l_a is the distance from the leading edge of the frond to the base of the pneumatocyst, l_b is the distance from the base of the pneumatocyst to the top of pneumatocyst, and l_c is the distance from the leading edge of the frond to the top of the pneumatocyst (Fig. 2).

The reconfiguration of and drag on each frond and pneumatocyst were measured during three tows in their unmanipulated state (i.e., not stiffened or punctured) and during three tows after manipulation. After the control and treatment measurements were made, the pneumatocyst was removed from the frond to measure drag on the frond by itself (3 times for each frond). The drag coefficient C_D of the pneumatocysts was calculated by:

$$C_D = \frac{2F_p}{\rho A u^2} \tag{2}$$

where F_p is the drag on the pneumatocyst by itself (i.e., drag on pneumatocyst and frond minus the drag on frond), ρ is the density of the water in the tow tank (998 kg m^{-3} at 20 °C, Vogel, 1994), A is the planform area of the pneumatocyst, and u is the tow velocity. Planform area was measured to the nearest 0.01 cm^2 using ImageJ. The drag forces on pneumatocysts before and after their respective manipulations were compared using paired t-tests.

The buoyancy forces of intact pneumatocysts were measured by removing them from the frond and using a spring scale to measure the force required to submerge each pneumatocyst in water. The planform areas of the pneumatocysts were measured to the nearest 0.01 cm^2 using ImageJ.

2.3. Force to pull a pneumatocyst off a frond

The force required to detach a pneumatocyst from the rachis was measured with an Instron materials testing machine (Model 5544, Norwood, MA, USA). The Instron machine pulled a nylon cord that was loosely tied around the pneumatocyst's petiole (strain rate = 20 mm min^{-1}). The rachis was held in place with a clamp and the force required to separate the pneumatocyst from it was recorded to the nearest 0.01 N (Fig. 2C). Sections of fronds bearing pneumatocysts were kept moist in air between 4 and 10 °C until they were tested in air at 20 °C; tests only lasted 2 min, so specimens remained cool. Planform areas of pneumatocysts were measured to the nearest 0.01 cm^2 using ImageJ.

2.4. Physical models to test the effect of pneumatocyst location on frond height

Physical models of flexible fronds were videotaped in a wave tank (described above in Section 2.2) to test the effect of pneumatocyst location along a frond on the height of the frond in the water. Physical models, instead of real *E. menziesii* fronds, were used because of the size limitation of the wave tank. Models of fronds were constructed of flagging tape (Presco, Sherman, TX, USA) with pneumatocysts that were air-filled silicon spheres, approximately 1 cm in diameter (H & P Sales, Vista, CA, USA). The flagging tape was negatively buoyant in fresh water; its mass density was 1455 kg m^{-3} and its flexural stiffness was 3.27 × 10^{-9} N m^2 (see Suppl. Material).

Model fronds were 30.0 cm long and 2.5 cm wide, and a pair of model pneumatocysts was attached by thread at 10, 20, or 30 cm from the frond base. The locations of pneumatocysts on the models represented real fronds with pneumatocysts at the tip, middle, or bottom of the frond. Models with no pneumatocysts were also made. Five replicate models of each configuration were constructed.

Models were scaled to be dynamically-similar to fronds of *E. menziesii* in waves in the field. Models were attached to the bottom of a paddle-driven wave tank (working section with a cross-section 30 × 30 cm and a length parallel to the flow of 100 cm; Hunter, 1988). At rest, the water in the wave tank was 20 cm deep. The ratio of model length to water depth (3:2) was similar to that of *E. menziesii* fronds in shallow surge channels. The wave tank paddle was driven at 0.24 and 0.07 Hz, producing waves with maximum horizontal water velocities of 0.296 m s^{-1} and 0.078 m s^{-1}, respectively. The ratio of the model length to the distance that the water traveled before reversing for both tank settings was approximately 1:1, which mimicked that of the real fronds in the field (see Section 2.5 below).

Each model was videotaped using a Fastec video camera at 20 fps at each wave frequency. In each frame of the video of a full wave cycle, the height of the distal end of each model above the substratum was measured to the nearest 1 mm with ImageJ. The time-averaged height of each model was determined, and the mean of those heights for the five replicate models of each configuration was calculated. The model heights were compared between the two wave frequencies using Mann-Whitney U tests.

2.5. Movement of *E. menziesii* fronds in wave-driven flow in the field

The effects of pneumatocysts on horizontal frond movement were tested by measuring the water velocity relative to *E. menziesii* fronds in a surge channel at HC in October 2013. Seven *E. menziesii* fronds were haphazardly collected from separate holdfasts near the surge channel and the proximal ends were cut off so that each frond tested was 1.5 m in length. The pneumatocysts found on each frond were located within the distal-most half of the frond. The diameters of the pneumatocysts were measured with calipers to the nearest 0.1 mm. The proximal end of each frond was anchored to the bottom of a surge channel using a brick, and the distal end of the frond was marked with surveyor's tape (3M, Saint Paul, MN, USA). The surge channel was approximately 1 m wide, 5 m long, and 1 m deep.

The water flow in the surge channel was measured while the motions of each kelp frond were videotaped. An acoustic Doppler velocimeter (ADV; SonTek 16-MHz MicroADV, San Diego, CA, USA) was placed at the mouth of the surge channel to measure water velocity to the nearest 0.01 cm s^{-1} as a function of time (sampling rate of 25 Hz) at a height of 20 cm above the substratum. A digital camera (Casio Exilim EX-F1, Dover, NJ, USA) was positioned above the channel with the horizontal component of its field of view parallel to the long axis of the surge channel so that the full range of frond motion was visible to the camera.

The movement of each frond in the surge channel was videotaped for 2 min (frame rate of 30 fps) with simultaneous ADV measurements of the ambient water velocities in the surge channel. Water velocities and frond movements were recorded for each frond with its naturally-occurring pneumatocysts, and then recorded again after all pneumatocysts were removed. In each video, the horizontal position of the frond's distal end was tracked to the nearest 0.1 cm using ImageJ and the velocities of the frond were calculated from the position data. Time series of the frond and water velocities were paired by averaging data into 0.2 s bins. Water velocities relative to the frond were calculated by subtracting the frond velocity from the water velocity in each bin, and then those data were sorted by the instantaneous ambient water speed in intervals of 1 cm s^{-1}. Next, the relative water velocities that each frond experienced, with and without its pneumatocysts, were compared among all the fronds at each instantaneous ambient water velocity using paired t-tests. The relative water velocities experienced by the fronds, with and without pneumatocysts, were compared across the entire range of instantaneous ambient water velocities using an analysis of covariance.

2.6. Frond height in the water column in waves in the field

The effect of pneumatocysts and ambient water velocity on the vertical position of fronds in the water column was tested using the same water velocity data and videotapes described in the previous section (Section 2.5). Each frame of the videos was scored for whether or not any part of a frond floated at the water's surface (1 = frond floating at the water surface, 0 = frond submerged below the water surface). Time series of the floating scores and ambient water speeds were paired by averaging data into 0.2 s bins and then sorted by the instantaneous ambient water speed in intervals of 1 cm s^{-1}. Within each binned ambient water speed, the proportion of time that each frond spent floating at the water's surface was determined for fronds both with and without their pneumatocysts. The probability that each frond floated at the water's surface, with and without its pneumatocysts, was compared at each instantaneous ambient water velocity using paired *t*-tests.

The density of frond tissue was measured at a consistent location on fronds, 45 cm from the terminal lamina (Fig. 1A), collected from HC following the field experiment. A circular piece of rachis, 5.50 mm in diameter, was cut from each frond using a hole punch. The thickness of the cut section was measured to the nearest 0.01 mm using digital calipers, and then the mass of the section was weighed to the nearest 0.001 g (wet weight after being patted dry with a paper towel) using a digital balance (AG245, Mettler Toledo, Columbus, OH, USA). These data were used to calculate the mass per volume of rachis tissue.

3. Results

3.1. Field surveys of pneumatocysts

Fronds with pneumatocysts were more common and occurred in larger numbers in summer than in winter. At all three sites (HC, MC, KB) in February, 10.5 to 11.3% of fronds longer than 10 cm had pneumatocysts, whereas in June, 10.6 to 49.1% of such fronds had pneumatocysts. On fronds bearing pneumatocysts in February, the mean number of pneumatocysts per length of frond ranged from 2.5 to 2.9 pneumatocysts m^{-1}, while in June there were 3.5 to 6.4 pneumatocysts m^{-1} (Fig. 3A, Table S1).

Pneumatocysts occurred over a wide range of locations on the fronds. Surveys of the locations of pneumatocysts on fronds at MW and MC in July 2017 showed that the most proximal pneumatocysts on each frond (i.e., closest to the holdfast) were at positions that ranged from 7 to 84% of the frond length from the base of the frond (i.e., the point where the frond branches from an older frond or from the holdfast). The most distal pneumatocysts were located at positions 36% to 99% of the frond length from the base. At MW, the median location of pneumatocysts, pooled across all surveyed fronds, was close to the frond midpoint (55% of the frond length from the base, n = 365 pneumatocysts from 30 fronds). At MC, the median location of pneumatocysts, pooled across all surveyed fronds, was also close to the frond's midpoint (51% of the frond length from the base, n = 261 pneumatocysts from 30 fronds) (Fig. 3B). There was no difference in the distribution of pneumatocyst location between fronds at MC and fronds at MW (Mann-Whitney *U* test, $p > 0.05$).

Pneumatocysts were larger at MC, the wave-exposed site, than at MW, the moderately wave-exposed site (Mann-Whitney U test, $p < 0.0005$, n = 839 pneumatocysts from MC, 409 from MW) (Fig. 3C).

3.2. Orientation of and drag on pneumatocysts

Buoyancy of the pneumatocyst and the stiffness of the petiole both affected the reorientation of pneumatocysts in flowing water and the drag on them. Pneumatocysts that were made neutrally buoyant leaned over more in flow and experienced lower drag than they did when they were positively buoyant (paired *t*-tests, $p < 0.005$, df = 14) (Fig. 4). In contrast, pneumatocysts with stiffened petioles were reoriented less by flow and experienced higher drag than they did without stiffened petioles (paired *t*-tests, $p < 0.005$, df = 16). The drag on a

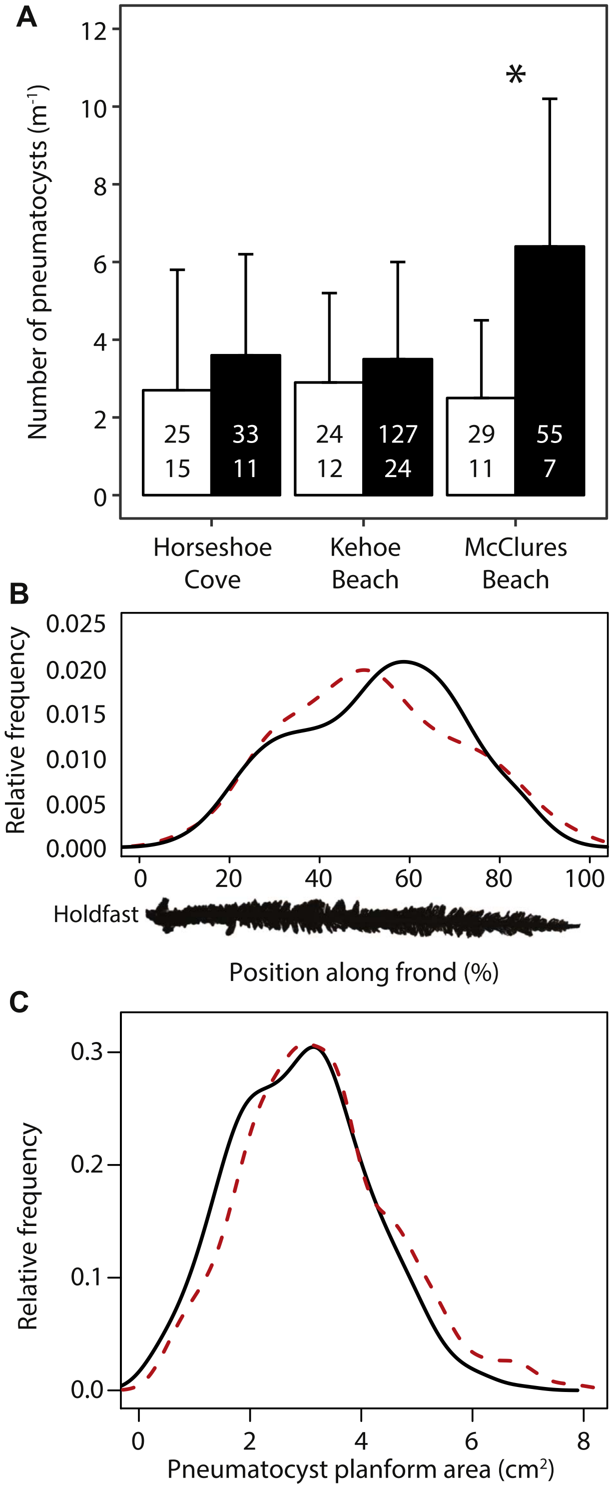

Fig. 3. (A) Pneumatocyst density (number of pneumatocysts per length of frond) of the pneumatocyst-bearing fronds on *E. menziesii* at three sites, sampled in winter (white bars) and the following summer (black bars). Error bars indicate 1 SD. There was a significant difference (indicated by an asterisk) between seasons at McClures Beach (Mann-Whitney *U* test, $p < 0.05$), but not for the other sites. The top value in each bar indicates the number of fronds measured, and the bottom value indicates the number of individual kelp whose fronds were measured. (B) Relative frequency of the locations of pneumatocysts along the length of fronds at Miwok Beach (black, solid line) and McClures Beach (red, dashed line), where 0% indicates the proximal part of the frond nearest the holdfast, and 100% indicates the tip of the frond. (C) Relative frequency of pneumatocyst size (planform area) at Miwok Beach (black, solid line) and McClures Beach (red, dashed line). At McClures Beach, the median pneumatocyst size was 3.11 cm^2 (range = 0.39 to 8.02, n = 839), and at Miwok Beach, the median pneumatocyst size was 2.93 cm^2 (range = 0.15 to 6.89, n = 409). (For interpretation of the references to colour in this figure legend, the reader is referred to the web version of this article.)

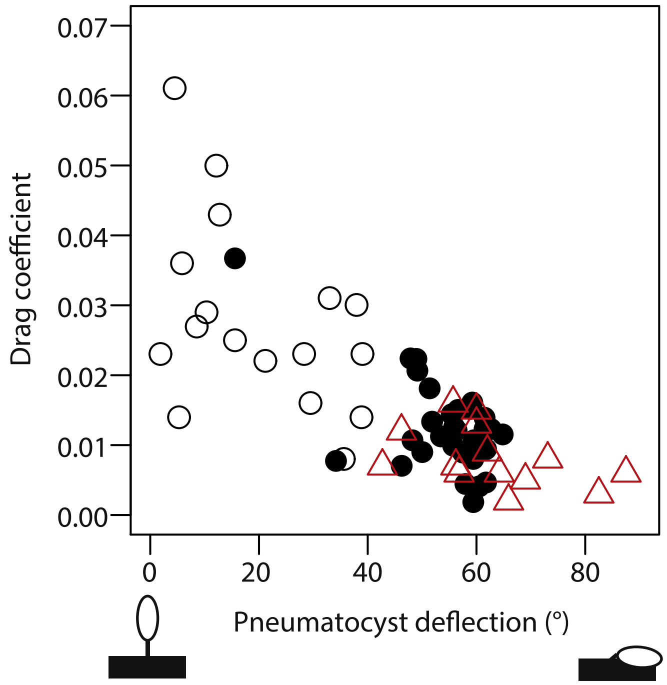

Fig. 4. Drag coefficients (Eq. (2)) of pneumatocysts were negatively correlated with pneumatocyst deflection (Eq. (1), Fig. 2B) in moving water (linear regression, $y = -0.0004x + 0.0360$, $p < 0.005$, $r^2 = 0.56$). Open circles indicate pneumatocysts that were positively buoyant with stiffened petioles, closed circles indicate pneumatocysts that were positively buoyant with flexible petioles (i.e., unmanipulated), and red open triangles indicate pneumatocysts that were neutrally buoyant with flexible petioles. (For interpretation of the references to colour in this figure legend, the reader is referred to the web version of this article.)

pneumatocyst was negatively correlated to the deflection of the pneumatocyst in flow (Fig. 4).

Unmanipulated pneumatocysts had a mean drag coefficient of 0.013 (SD = 0.007, n = 32) and a mean deflection angle (Fig. 2B) of 54.65° (SD = 9.44, n = 33) (Fig. 4). Buoyancy was positively correlated to the planform area of pneumatocysts. Buoyant forces ranged between 0.40 and 1.74 mN for pneumatocysts between 0.70 and 6.60 cm^2 in planform area (Fig. 5A). Drag was smaller than buoyancy for the majority of the unmanipulated pneumatocysts (Fig. 5B).

3.3. *Force to remove pneumatocysts from the frond*

The force to remove a pneumatocyst from a frond was positively correlated to the planform area of the pneumatocyst (Fig. 6). Detachment forces ranged from 3.91 to 35.63 N for pneumatocysts between 0.77 and 8.64 cm^2 in planform area.

3.4. *Physical models to test the effect of pneumatocyst location on frond height*

The heights of model fronds above the substratum of a laboratory wave tank were affected by the positions of pneumatocysts and by the wave action. For both wave regimes tested, fronds exposed to the oscillatory flow of waves remained, on average, higher in the water column when the pneumatocysts were located at the distal tip of a frond than when they were at more proximal positions (Fig. 7). Fronds with pneumatocysts located at their midpoint or proximal end were higher in the water column when exposed to the high velocity, high frequency waves than when exposed to the slower low frequency waves (Mann-Whitney *U* tests, $p < 0.05$, n = 5 replicates of each pneumatocyst position in each wave condition). In contrast, the height of fronds with pneumatocysts at the distal tip, and for fronds without pneumatocysts, did not differ between the two wave conditions that we tested (Mann-Whitney U tests, $p > 0.05$, n = 5 replicates of in each wave condition).

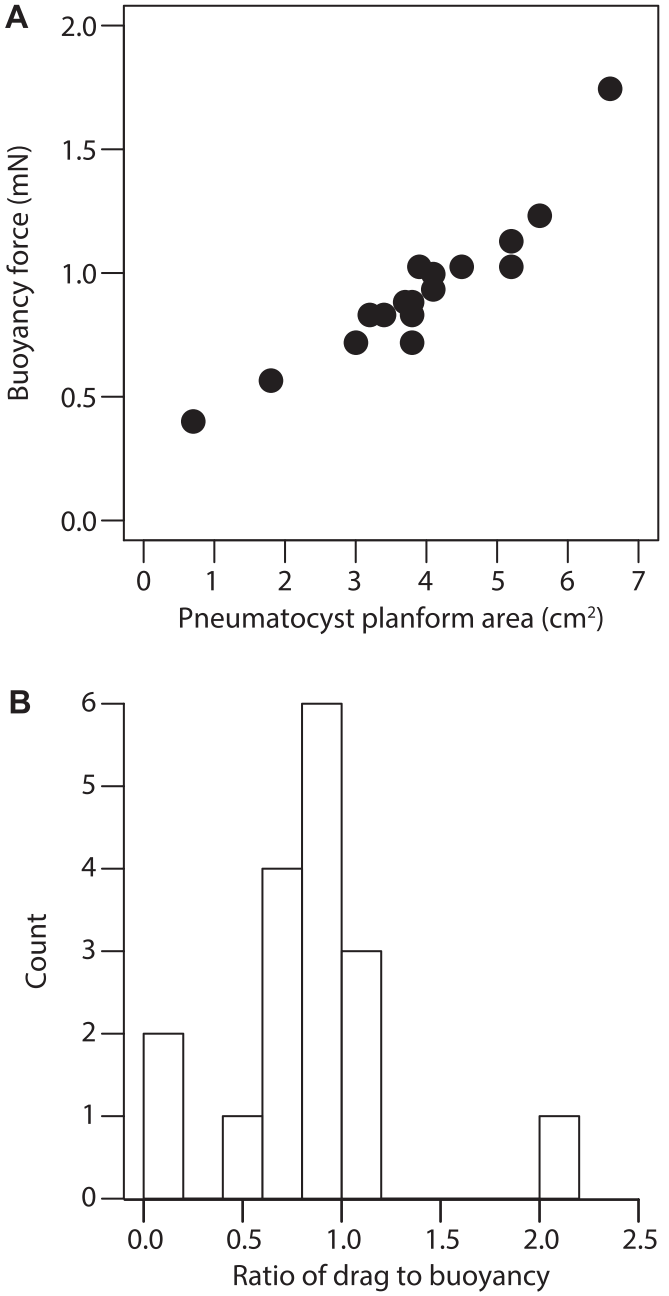

Fig. 5. (A) Buoyancy of pneumatocysts was positively correlated to the planform area of the pneumatocysts (linear regression, $y = 0.198x + 0.156$, $p < 0.005$, $r^2 = 0.86$). (B) The number of pneumatocysts towed at a mean velocity of 0.58 $\mathrm{m\,s^{-1}}$ (SD = 0.03, n = 17) that had different ratios of drag to buoyancy (median = 0.91, minimum = 0.13, maximum = 2.03).

3.5. *Frond movement in wave-driven flow in the field*

Fronds collected for the field experiments had between 3 and 21 pneumatocysts, and all pneumatocysts were between 7.5 and 20.0 mm in diameter. Fronds of *E. menziesii* moved back-and-forth with each wave (Fig. 8A), such that the water velocity relative to the frond surface was slower than the ambient water velocity (Fig. 8B). The presence of pneumatocysts only affected the relative water velocity past the distal ends of the fronds at three instantaneous ambient water velocities of

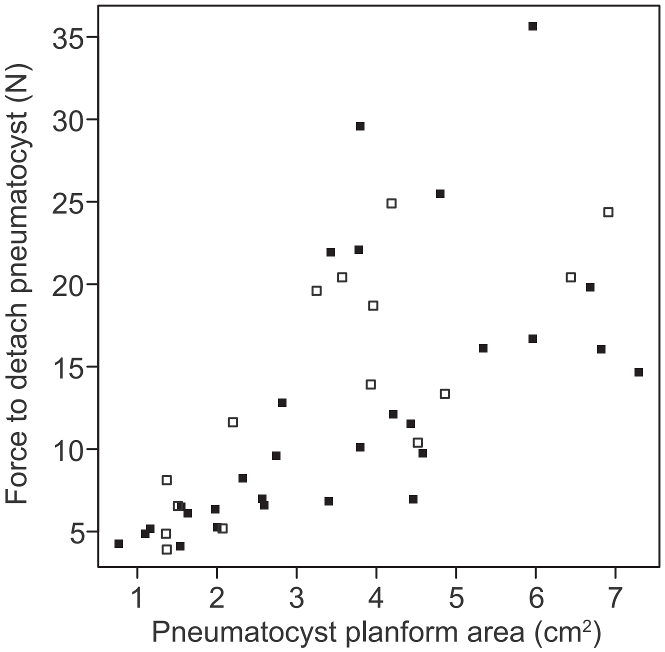

Fig. 6. The force to remove a pneumatocyst from a frond was positively correlated to the size of the pneumatocyst (linear regression, $y = 2.88x + 2.75$, $p < 0.005$, $r^2 = 0.48$). Filled black squares are pneumatocysts from the moderately wave-exposed site, Miwok Beach, and open red squares are pneumatocysts from the wave-exposed site, McClures Beach.

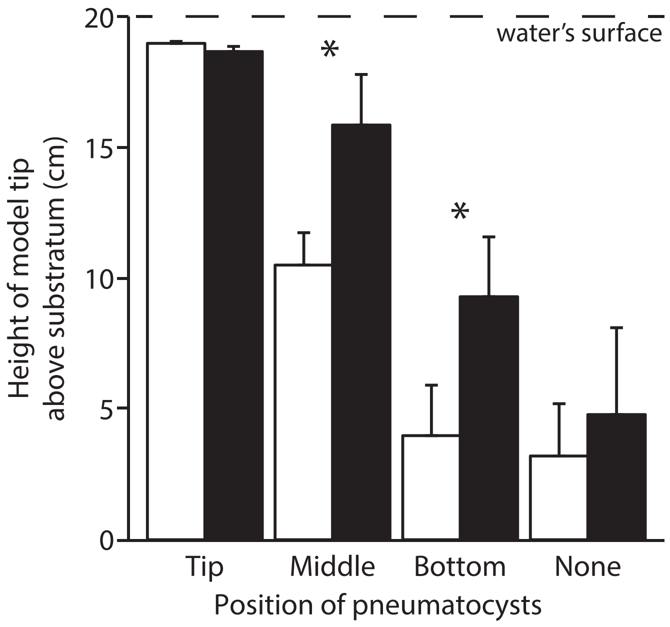

Fig. 7. Mean height of the tip above the substratum of physical models of fronds with pneumatocysts located at the tip, middle, or base of the frond, or with no pneumatocysts. White bars are for models in the slow, low-frequency waves, and black bars are for models in the fast, high-frequency waves (error bars show 1 SD, n = 5 frond models). Asterisks indicate models whose mean heights were significantly affected by the wave setting (Mann-Whitney *U* tests, $p < 0.05$).

-32, -30, and -1 cm s^{-1} (paired *t*-tests, $p < 0.05$, df > 3), which, all being negative velocities, indicate water movement in the seaward direction. All fronds, regardless of pneumatocysts, experienced approximately 82 to 83% of the instantaneous ambient water velocities -36 to 50 cm s^{-1} (Fig. 8B, C).

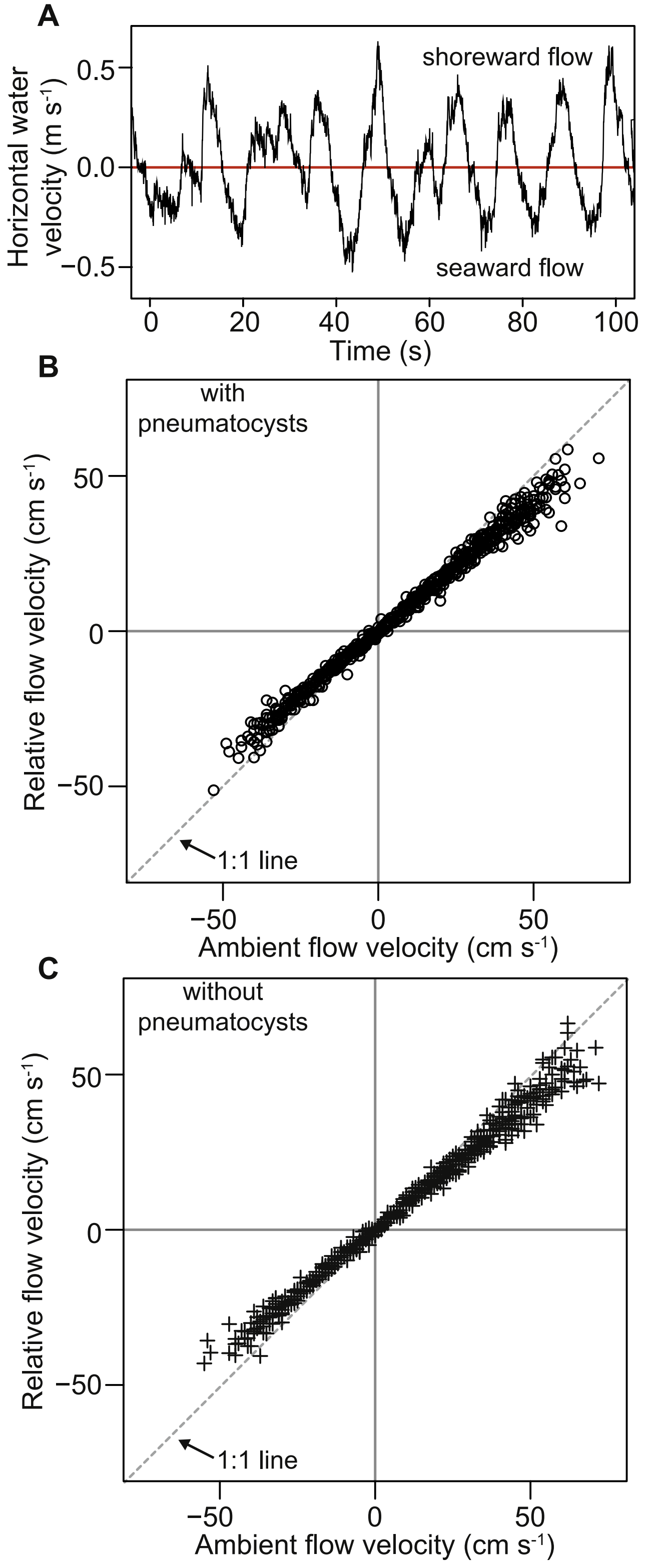

(caption on next page)

3.6. *Frond height in water column in the field*

In ambient water speeds from 0 to 40 cm s^{-1}, fronds with pneumatocysts spent more time floating at the air-water interface than did fronds without pneumatocysts (paired *t*-tests, $p < 0.05$, df > 4; Fig. 9). Even with pneumatocysts, the probability of a frond floating at the water surface decreased with increasing ambient water speed,

Fig. 8. (A) Horizontal velocity plotted as a function of time for the back-and-forth flow of waves in a surge channel. Velocities above the red line indicate shoreward flow and velocities below the red line indicate seaward flow. (B) Instantaneous water flow velocities relative to the tips of fronds with pneumatocysts (data for 7 fronds pooled) plotted at a function of instantaneous ambient flow velocity (rounded off to the nearest 1 cm s^{-1}). The dashed gray line is a 1:1 line for reference. (C) Instantaneous flow velocities relative to fronds without pneumatocysts (data for 7 fronds pooled) plotted at a function of instantaneous ambient flow velocity. The dashed gray line is the same as in B. There were no differences in the relative flow velocities for fronds with and without pneumatocysts across the range of ambient flow velocities measured (analysis of covariance, $p > 0.05$, covariate = ambient flow velocity, factor = presence of pneumatocysts). All frond tips experienced instantaneous water velocities relative to their surfaces that were 82 to 83% of the instantaneous ambient flow velocity (linear regression for fronds with pneumatocysts, $y = 0.83x - 0.01$, $p < 0.005$, $r^2 = 0.99$; linear regression for fronds without pneumatocysts, $y = 0.82x + 0.25$, $p < 0.005$, $r^2 = 0.99$). (For interpretation of the references to colour in this figure legend, the reader is referred to the web version of this article.)

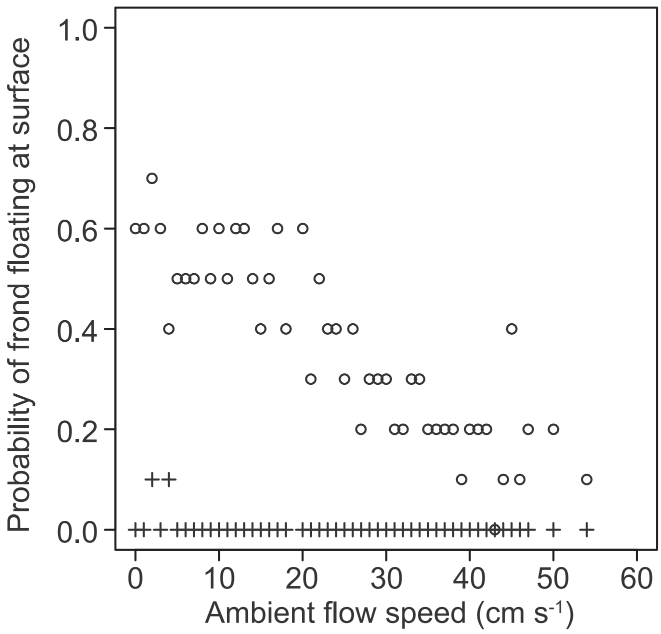

Fig. 9. Probability of fronds floating at the water's surface (i.e., air-water interface) at instantaneous ambient flow speeds from 0 to 54 cm s^{-1}. Open circles are fronds with pneumatocysts and crosses are fronds without pneumatocysts. The probability of floating for fronds with pneumatocysts was negatively correlated to ambient flow speed (linear regression, $y = -0.01x + 0.62$, $p < 0.005$, $r^2 = 0.76$).

whereas fronds without pneumatocysts were only observed floating at the water surface in very slow ambient water speeds of 2 and 4 cm s^{-1} (Fig. 9). The mass density of frond rachis tissue in the middle of the frond (45 cm from the intercalary meristem) was 1092 kg m^{-3} (SD = 74, n = 5), which is greater than that of sea water (1024 kg m^{-3} at 20 °C; Vogel, 1994), so fronds without pneumatocysts sink in still water.

4. Discussion

4.1. Reorientation of individual pneumatocysts in flow reduces drag

Reconfiguration of seaweeds in moving water has mostly been studied on the scale of the entire organism (Stewart, 2006a; Martone et al., 2012), whereas the focus of the present study was on the reconfiguration of pneumatocysts relative to the fronds of *Egregia menziesii* when in flow. Pneumatocysts floats are rigid, but the petioles can bend easily, so reconfiguration of the structure was limited to bending at the petiole such that the pneumatocyst leaned over closer to the rachis to a mean deflection (Fig. 2B) of 54.65° in a current of 0.58 m s^{-1} (Fig. 4). This deflection is in contrast to the reconfiguration of flexible leaves on terrestrial plants, which fold into cones and bend at the petiole (Vogel, 1989), or to the flexible thalli of seaweeds, the blades of which can be folded into streamlined shapes (Carrington, 1990; Martone et al., 2012) or pushed together into streamlined bundles (Koehl and Alberte, 1988). However, deflection by bending at the petiole was sufficient to reduce drag on the pneumatocysts, and consequently the pneumatocysts produced more buoyancy than they did drag (Fig. 5B). The buoyancy of the pneumatocyst is antagonistic to the flexibility of the petiole, and actually inhibits reconfiguration of the pneumatocyst to some degree (Fig. 4). This trade-off between flexibility and buoyancy has been shown for the entire thallus of the seaweed *Turbinaria ornata* (Stewart, 2006a), but not for individual structures on a seaweed.

The drag at field-relevant velocities of 0.58 m s^{-1} and the buoyant forces on the pneumatocysts were each < 2 mN (Fig. 5), yet the force to break a pneumatocyst from the frond ranged from 3 to 36 N (Fig. 6). These measurements indicate that intact pneumatocysts can resist drag and buoyant forces at least 1000 times greater than those they are likely to experience in the field, whereas the frond itself is approximately 12 times stronger than the hydrodynamic forces it is expected to encounter in nature (Friedland and Denny, 1995). Other factors can cause pneumatocysts to be weakened and break from the frond, such as herbivory or abrasion against rocks (Black, 1976; Lowell et al., 1991). Such pneumatocyst loss is probably a factor in producing the wide range of pneumatocyst numbers and locations on fronds measured in the field (Fig. 3A, B).

4.2. Effects of pneumatocysts on drag and photosynthesis

The magnitude of the drag on a pneumatocyst measured in this study is approximately three to four orders of magnitude lower than the total drag on an entire *E. menziesii* (e.g., Gaylord et al., 2008). It is likely that fronds of *E. menziesii* can have a wide variety of pneumatocyst sizes and numbers without paying a price in increased hydrodynamic drag. Our drag measurements were made in back-and-forth flow in the wave tank that corresponds to the oscillating flow encountered by *E. menziesii* at times in the tidal cycle when it is either shoreward or seaward of breaking waves. Martone et al. (2012) found that hydrodynamic forces on algal blades exposed to breaking waves were higher than those measured in a flume, which suggests that the forces on *E. menziesii* in breaking waves would also be higher than those we measured. Despite this, kelp at the wave-exposed site had larger and more numerous pneumatocysts than kelp at the moderately wave-exposed site (Fig. 3C). The differences in pneumatocyst size and number between wave exposures suggest that the benefit of buoyancy from pneumatocysts is more important than the problem of increased drag due to pneumatocysts, but these differences also correlate to the decreased herbivory and increased thallus sizes observed for kelp at sites with heavy wave exposure (Smale et al., 2016; Burnett, 2017).

Pneumatocysts may indirectly affect the growth of the kelp. Even though pneumatocysts have lower photosynthetic rates than do the vegetative lateral blades on *E. menziesii* fronds (Henkel and Murray, 2007), they probably enhance the overall photosynthetic rate of a frond by holding it high in the water column (Fig. 7) where photon flux density is greater than at depth (e.g., Rohde et al., 2008; Colvard et al., 2014). Furthermore, buoyant seaweeds in dense aggregations encounter more light than do non-buoyant individuals (Stewart et al., 2007). The flexibility of fronds that allows them to be moved around relative to each other by turbulent waves, coupled with the buoyancy of fronds with pneumatocysts, permits *E. menziesii* to have numerous fronds and to grow in dense aggregations near other individuals without their fronds being continuously shaded by neighboring fronds. Koehl and Alberte (1988) found that motions of ruffled blades of the kelp *Nereocystis luetkeana* in flowing water reduced self-shading, thereby enhancing photosynthetic rate. Growing in dense aggregations also reduces the hydrodynamic forces that the individual kelp or fronds experience in waves or currents (Holbrook et al., 1991; Johnson, 2001; Stewart et al., 2007), suggesting that any increase in drag from pneumatocysts on an individual frond may be counteracted by the fronds growing in dense aggregations.

4.3. Interaction of flexibility and buoyancy

Flexibility reduces hydrodynamic forces on seaweeds by allowing them to "go with the flow" in waves and to be bent over parallel to ambient water flow and reconfigured into streamlined shapes, whereas buoyancy enables them to hold photosynthesizing tissues high in the water column. The reduction in drag that flexibility provides and the effect that buoyancy has on drag depend on the flow regime and the size of the seaweed. In wave-driven flow, a flexible seaweed that is buoyant is able to reconfigure with the oncoming wave and then rebound to an upright posture when the flow slows (Stewart, 2004, 2006a). If a seaweed is short relative to the distance that the water travels in each wave before it reverses direction, then the seaweed fully reconfigures in the flow and is exposed to a period of unidirectional flow relative to its surfaces, similar to seaweeds that are exposed to unidirectional currents. In unidirectional flow, the buoyancy of a flexible body attached to a surface resists the body's ability to be bent over by the current, which can lead to higher drag than if it were not buoyant (as was measured for individual pneumatocysts, Fig. 4). Buoyant seaweeds that are short (length ≪ distance of water travel in a wave) and that live in habitats exposed to waves, such as *Turbinaria ornata*, can experience a similar buoyancy-induced increase in drag compared with non-buoyant seaweeds (Stewart, 2006a). In contrast, for long seaweeds such as *E. menziesii* that can move with the flow for most or all of a wave cycle, the penalty of increased hydrodynamic force due to buoyancy is very small. Waves must move water greater distances (i.e., must have longer periods and higher peak velocities) to expose long seaweeds to the drag penalty of buoyancy than to subject short seaweeds to that penalty. For example, in the present study *E. menziesii* moved at 17% of the ambient water velocity in water velocities up to $0.5\ \mathrm{m\ s^{-1}}$, experiencing a *relative* water velocity that was 83% of the ambient water velocity (Fig. 8B). If a wave moved water at a constant velocity of $0.5\ \mathrm{m\ s^{-1}}$ (i.e., the peak velocity of waves observed in the surge channel at Horseshoe Cove, Fig. 8A), the wave would still need to push water for > 17 s (i.e., almost twice the wave period of normal waves, www.ndbc.noaa.gov) for a 1.5 m frond to be fully reconfigured in the flow ($1.5\ \mathrm{m} / [0.17 \times 0.5\ \mathrm{m\ s^{-1}}]$) (Fig. 8A). Thus, long buoyant kelp can avoid a buoyancy-induced drag penalty in habitats exposed to larger waves than can short seaweeds.

4.4. Flexible, floating fronds provide habitat to other organisms

Being flexible and positively buoyant allows kelp to grow to large sizes and in dense aggregations that make it an important habitat-forming organism in marine systems (Stenneck et al., 2002). *E. menziesii* is preferred over other macroalgal species as habitat and food by many herbivores due to its palatability and the protection it offers to invertebrate epifauna (Leighton, 1971; Sotka, 2007). The pneumatocysts allow the kelp to grow numerous fronds in close proximity to each other (Burnett, 2017) without completely shading each other out (Stewart et al., 2007). Dense aggregations of fronds, either from single or multiple individuals, can reduce the velocity of water flow around and through the kelp canopy (Eckman, 1983; Gaylord et al., 2007), and lower the risk of large epifauna (e.g., amphipods, crabs) being dislodged by hydrodynamic forces (Fenwick, 1976; Duggins et al., 2001). Additionally, the complex three-dimensional arrangement of numerous fronds can provide increased surface area and interstitial volume for epibiota to colonize, enhancing the kelp's ecological role as a source of habitat and food (Norderhaug et al., 2007; Norderhaug and Christie, 2011). The flexibility of the fronds allows the kelp to reduce the hydrodynamic forces it experiences from waves (Koehl, 1984, 1986), such that the kelp and the vital habitat it provides are better able to persist through periods of large waves.

In addition to providing habitat on its fronds, *E. menziesii* can alter the surrounding benthic habitat by scouring and shading the substratum, processes that are enabled by the fronds' flexibility and buoyancy (Arkema et al., 2009; Hughes, 2010). During immersion at high tide, the back-and-forth water motion of waves can drag the fronds along the substratum, dislodging animals, as well as seaweeds, and removing sediment (Kennelly, 1989; Hughes, 2010). Floating *E. menziesii* canopies, or canopies at rest on the substratum at low tide, can shade and consequently reduce the abundance of small algae living below the kelp (Arkema et al., 2009). Shading and scouring together can not only dislodge or kill benthic organisms, but also result in entire shifts of the benthic community's structure (e.g., dominated by invertebrate suspension-feeders rather than seaweeds) (Kennelly, 1989; Arkema et al., 2009; Hughes, 2010). This cascade of ecological effects is made possible by the buoyant pneumatocysts on *E. menziesii* that permit the kelp to have long, flexible fronds, and these ecological effects would likely not occur if the kelp relied on stiffness rather than buoyancy to stay upright (e.g., Gaylord and Denny, 1997).

Our results for *E. menziesii* indicate that pneumatocysts on macroalgae in wave-swept habitats increase the hydrodynamic forces on the seaweeds by only a small amount, but permit those macroalgae to be long and flexible. Although pneumatocysts at frond tips are most effective at holding kelp high in the water column, only a few pneumatocysts at any locations along a frond are capable of enhancing the frond's height in waves. Remaining upright in the water column helps the kelp grow to large sizes, enabling *E. menziesii* to be a dominant habitat-forming organism in the wave-swept rocky intertidal zones on the west coast of North America.

Acknowledgements

This work was supported by a National Science Foundation Integrative Graduate Education and Research Training Grant DGE-0903711 (to R. Full, M. Koehl, R. Dudley and R. Fearing), a National Science Foundation Graduate Research Fellowship DGE-1106400 to N. Burnett, and a 2014 Point Reyes Fund for Marine Science to N. Burnett. E. Armstrong, A. Belk, W. Kumler, R. Romero, and R. Tanner assisted with the field components of this study.

Appendix A. Supplementary data

Supplementary data to this article can be found online at http://dx.doi.org/10.1016/j.jembe.2017.09.003.

References

Abbott, I.A., Hollenberg, G.J., 1976. Marine Algae of California. Stanford University Press, Stanford, CA.

Arkema, K.K., Reed, D.C., Schroeter, S.C., 2009. Direct and indirect effects of giant kelp determine benthic community structure and dynamics. Ecology 90, 3126–3137.

Bertness, M.D., Crain, C.M., Silliman, B.R., Bazterrica, M.C., Reyna, M.V., Hildago, F., Farina, J.K., 2006. The community structure of western Atlantic Patagonian rocky shores. Ecol. Monogr. 76, 439–460.

Black, R., 1976. The effects of grazing by the limpet, *Acmaea insessa*, on the kelp, *Egregia laevigata*, in the intertidal zone. Ecology 57, 265–277.

Burnett, N.P., 2017. The Effects of Turbulent Wave-driven Water Motion on Interactions of the Intertidal Kelp *Egregia menziesii* With Its Herbivores (PhD dissertation). University of California, Berkeley, CA.

Carrington, E., 1990. Drag and dislodgment of an intertidal macroalga: consequences of morphological variation in *Mastocarpus papillatus* Kutzing. J. Exp. Mar. Biol. Ecol. 139, 185–200.

Christie, H., Norderhaug, K.M., Fredriksen, S., 2009. Macrophytes as habitat for fauna. Mar. Ecol. Prog. Ser. 396, 221–233.

Colvard, N.B., Carrington, E., Helmuth, B., 2014. Temperature-dependent photosynthesis in the intertidal alga *Fucus gardneri* and sensitivity to ongoing climate change. J. Exp. Mar. Biol. Ecol. 458, 6–12.

Demes, K.W., Pruitt, J.N., Harley, C.D.G., Carrington, E., 2013. Survival of the weakest: Increased frond mechanical strength in a wave-swept kelp inhibits self-pruning and increases whole-plant mortality. Funct. Ecol. 27, 439–445.

Denny, M.W., 1988. Biology and the Mechanics of the Wave-swept Environment. Princeton University Press, Princeton.

Denny, M.W., 1995. Predicting physical disturbance: mechanistic approaches to the study of survivorship on wave-swept shores. Ecol. Monogr. 65, 371–418.

Denny, M.W., Gaylord, B.P., Helmuth, B., Daniel, T., 1998. The menace of momentum: dynamic forces on flexible organisms. Limnol. Oceanogr. 43, 955–968.

Duggins, D., Eckman, J.E., Siddon, C.E., Klinger, T., 2001. Interactive roles of mesograzers and current flow in survival of kelps. Mar. Ecol. Prog. Ser. 223, 143–155.

Eckman, J.E., 1983. Hydrodynamic processes affecting benthic recruitment. Limnol. Oceanogr. 28, 241–257.

Fenwick, G.D., 1976. The effect of wave exposure on the amphipod fauna of the alga *Caulerpa brownii*. J. Exp. Mar. Biol. Ecol. 25, 1–18.

Friedland, M.T., Denny, M.W., 1995. Surviving hydrodynamic forces in a wave-swept environment: consequences of morphology in the feather boa kelp, *Egregia menziesii* (Turner). J. Exp. Mar. Biol. Ecol. 190, 109–133.

Gaylord, B., 1999. Detailing agents of physical disturbance: wave-induced velocities and accelerations on a rocky shore. J. Exp. Mar. Biol. Ecol. 239, 85–124.

Gaylord, B., Denny, M.W., 1997. Flow and flexibility I. Effects of size, shape and stiffness in determining wave forces on the stipitate kelps *Eisenia arborea* and *Pterygophora californica*. J. Exp. Biol. 200, 3141–3164.

Gaylord, B., Denny, M.W., Koehl, M.A.R., 2003. Modulation of wave forces on kelp canopies by alongshore currents. Limnol. Oceanogr. 48, 860–871.

Gaylord, B., Rosman, J.H., Koseff, J.R., Fram, J., MacIntyre, S., Arkema, K., McDonald, C., Brzezinski, M.A., Largier, J.L., Monismith, S.G., Raimondi, P.T., Mardian, B., 2007. Spatial patterns of flow and their modification within and around a giant kelp forest. Limnol. Oceanogr. 52, 1838–1852.

Gaylord, B., Denny, M.W., Koehl, M.A.R., 2008. Flow forces on seaweeds: field evidence for roles of wave impingement and organism inertia. Biol. Bull. 215, 295–308.

Graham, M.H., 2004. Effects of local deforestation on the diversity and structure of southern California giant kelp forest food webs. Ecosystems 7, 341–357.

Henkel, S.K., Murray, S.N., 2007. Reproduction and morphological variation in southern California populations of the lower intertidal kelp *Egregia menziesii* (Laminariales). J. Phycol. 43, 242–255.

Holbrook, N.M., Denny, M.W., Koehl, M.A.R., 1991. Intertidal "trees": consequences of aggregation on the mechanical and photosynthetic properties of sea-palms *Postelsia palmaeformis* Ruprecht. J. Exp. Mar. Biol. Ecol. 146, 39–67.

Hughes, B.B., 2010. Variable effects of a kelp foundation species on rocky intertidal diversity and species interactions in central California. J. Exp. Mar. Biol. Ecol. 393, 90–99.

Hunter, T., 1988. Mechanical Design of Hydroids: Flexibility, Flow Forces, and Feeding in *Obelia longissima* (Doctoral dissertation). University of California, Berkeley, California (228 pp.).

Johnson, A.S., 2001. Drag, drafting, and mechanical interactions in canopies of the red alga *Chondrus crispus*. Biol. Bull. 201, 126–135.

Johnson, S.Y., Dartnell, P., Golden, N.E., Hartwell, S.R., Erdey, M.D., Greene, H.G., Cochrane, G.R., Kvitek, R.G., Manson, M.W., Endris, C.A., Dieter, B.E., Watt, J.T., Krigsman, L.M., Sliter, R.W., Lowe, E.N., Chin, J.L., 2015a. California state waters map series-offshore of Bodega Head, California. In: Johnson, S.Y., Cochran, S.A. (Eds.), U.S. Geological Survey Open-file Report 2015–1140, http://dx.doi.org/10.3133/ofr20151140.

Johnson, S.Y., Dartnell, P., Golden, N.E., Hartwell, S.R., Greene, H.G., Erdey, M.D., Cochrane, G.R., Watt, J.T., Kvitek, R.G., Manson, M.W., Endris, C.A., Dieter, B.E., Krigsman, L.M., Sliter, R.W., Lowe, E.N., Chin, J.L., 2015b. California state waters map series-offshore of Tomales Point, California. In: Johnson, S.Y., Cochran, S.A. (Eds.), U.S. Geological Survey Open-file Report 2015–1088, http://dx.doi.org/10.3133/ofr20151088.

Kennelly, S.J., 1989. Effects of kelp canopies on understorey species due to shade and scour. Mar. Ecol. Prog. Ser. 50, 215–224.

Koehl, M.A.R., 1984. How do benthic organisms withstand moving water? Am. Zool. 24, 57–70.

Koehl, M.A.R., 1986. Seaweeds in moving water: form and mechanical function. In: Givnish, T.J. (Ed.), On the Economy of Plant Form and Function. Cambridge University Press, Cambridge, pp. 603–634.

Koehl, M.A.R., Alberte, R.S., 1988. Flow, flapping, and photosynthesis of *Nereocystis luetkeana*: a functional comparison of undulate and flat blade morphologies. Mar. Biol. 99, 435–444.

Koehl, M.A.R., Wainwright, S.A., 1977. Mechanical adaptations of a giant kelp. Limnol. Oceanogr. 22, 1067–1071.

Krumhansl, K.A., Scheibling, R.E., 2012. Production and fate of kelp detritus. Mar. Ecol. Prog. Ser. 467, 281–302.

Leighton, D.L., 1971. Grazing activities of benthic invertebrates in southern California kelp beds. In: North, W.J. (Ed.), The Biology of Giant Kelp Beds (*Macrocystis*) in California. Nova Hedwigia, pp. 421–453.

Lial, M.L., Hornsby, J., Schneider, D.I., 2009. Trigonometry. Pearson, Boston.

Lowell, R.B., Markham, J.H., Mann, K.H., 1991. Herbivore-like damage induces increased strength and toughness in a seaweed. Proc. R. Soc. London, Ser. B 243, 31–38.

Martone, P.T., Kost, L., Boller, M., 2012. Drag reduction in wave-swept macroalgae: alternative strategies and new predictions. Am. J. Bot. 99, 806–815.

Norderhaug, K.M., Christie, H., 2011. Secondary production in a *Laminaria hyperborea* kelp forest and variation according to wave exposure. Estuar. Coast. Shelf Sci. 95, 135–144.

Norderhaug, K.M., Christie, H., Fredriksen, S., 2007. Is habitat size an important factor for faunal baundances on kelp (*Laminaria hyperborea*)? J. Sea Res. 58, 120–124.

Rohde, S., Hiebenthal, C., Wahl, M., Karez, R., Bischof, K., 2008. Decreased depth distribution of *Fucus vesiculosus* (Phaeophyceae) in the Western Baltic: effects of light deficiency and epibionts on growth and photosynthesis. Eur. J. Phycol. 43, 143–150.

Smale, D.A., Burrows, M.T., Evans, A.J., King, N., Sayer, M.D.J., Yunnie, A.L.E., Moore, P.J., 2016. Linking environmental variables with regional-scale variability in ecological structure and standing stock of carbon within UK kelp forests. Mar. Ecol. Prog. Ser. 542, 79–95.

Sotka, E.E., 2007. Restricted host used by the herbivorous amphipod *Peramphithoe tea* is motivated by food quality and abiotic refuge. Mar. Biol. 151, 1831–1838.

Stenneck, R.S., Graham, M.H., Bourque, B.J., Corbett, D., Erlandson, J.M., Estes, J.A., Tegner, M.J., 2002. Kelp forest ecosystems: biodiversity, stability, resilience and future. Environ. Conserv. 29, 436–459.

Stewart, H.L., 2004. Hydrodynamic consequences of maintaining an upright posture by different magnitudes of stiffness and buoyancy in the tropical alga *Turbinaria ornata*. J. Mar. Syst. 49, 157–167.

Stewart, H.L., 2006a. Hydrodynamic consequences of flexural stiffness and buoyancy for seaweeds: a study using physical models. J. Exp. Biol. 209, 2170–2181.

Stewart, H.L., 2006b. Ontogenetic changes in buoyancy, breaking strength, extensibility, and reproductive investment in a drifting macroalga *Turbinaria ornata* (Phaeophyta). J. Phycol. 42, 43–50.

Stewart, H.L., Payri, C.E., Koehl, M.A.R., 2007. The role of buoyancy in mitigating reduced light in macroalgal aggregations. J. Exp. Mar. Biol. Ecol. 343, 11–20.

Underwood, A.J., Denley, E.J., Moran, M.J., 1983. Experimental analyses of the structure and dynamics of mid-shore rocky intertidal communities in New South Wales. Oecologia 56, 202–219.

Vogel, S., 1989. Drag and reconfiguration of broad leaves in high winds. J. Exp. Bot. 40, 941–948.

Vogel, S., 1994. Life in Moving Fluids. Princeton University Press.